

Cyclic loading effects on flexible-bonded soft-rigid granular mixes

Mehdi Alam^{1,2*}, Arghya Das², and Mahdi M Disfani¹

¹Department of Infrastructure Engineering, The University of Melbourne, 3010 Melbourne, Australia

²Department of Civil Engineering, Indian Institute of Technology Kanpur, 208016 Uttar Pradesh, India

Abstract. The mechanical response of flexible bonded soft (waste tyres)-rigid (crushed rock) is studied under cyclic loading. The use of waste tyres for different transportation infrastructure has attracted the attention of the engineers to understand the behaviour of these materials mixed with different geotechnical material like soil and crushed rock. Discrete Element Method (DEM) is employed to understand the behaviour. A coherent contact model is used in DEM with modelling strategy, developed for these materials. The contact parameters were calibrated against oedometric test responses for various mix combination. Two samples with varying soft contents are considered in this study, while keeping the binder content in the mix constant. The samples are subjected to strain and stress-controlled loading. The macroscopic stress-strain behaviour varies with changes in the soft and binder content percentages in the mix. The stress reduction for a strain-controlled test is higher for a mix containing higher soft content. Similarly for a stress-controlled test, the strain accumulation happens at a much higher rate for higher soft content mix. The current study involves loading beyond the yield. It is observed that stress reduction is influenced not only by the soft and binder content but also by bond breakage leading to stress reduction during the first loading cycle. Furthermore, a logarithmic function is proposed for both strain and stress-controlled tests to relate the modulus with the number of cycles.

1 Introduction

The use of waste tyre-based granular mix has gained the interest of researchers recently. However, the inclusion of soft particles, such as tyre leads to a reduction in the strength and stiffness of the mix. The addition of binders has proven to be an efficient solution to improve the properties of these mixes. In this study, a polyurethane-based binder, which is flexible in nature, is used. Experimental and numerical works have been performed for unbonded soft-rigid mixes, and their behaviour under different loading conditions is well known now [1–6]. These studies primarily focus on the mechanical response of soft-rigid mixes and their microstructural behaviour. However, there are only limited studies available for the bonded soft-rigid mixes. The available studies mainly deal with cemented mixes [7] rather than using flexible binders [8], which have a distinct advantage over rigid binders by allowing the deformation of the soft particles and forming reinforcement network; hence improving the durability of the mix. Moreover, rigid binders fracture upon reaching their peak stress, causing the mix to behave as unbonded beyond that point. The studies on the flexible bonded soft-rigid mixes mainly focus on one-dimensional testing[9]. However, the materials, if used as pavement materials, should be tested for their cyclic behaviour. In this study, both stress and strain-controlled cyclic oedometer tests are performed using

the Discrete Element Method (DEM) to assess the response of the mixes with flexible binders with varying two different percentages of the soft content in the mix.

2 DEM model

2.1 Contact model

For the current study, a contact model developed specifically for the mixtures of soft, rigid and flexible binder materials is used [9]. The normal (σ) and shear (τ) stresses at the bond periphery is calculated using Eq.1 where F_n, F_s are the normal and shear forces at the bond periphery respectively; M_b, M_t are the bending and twisting moments respectively and A, R, I, J are the cross-sectional parameters area, radius, moment of inertia and polar moment of inertial respectively.

$$\sigma = \frac{F_n}{A} + \frac{M_b/R}{I} \quad (1a)$$

$$\tau = \frac{F_s}{A} + \frac{M_t/R}{J} \quad (1b)$$

When the bond stress reaches the peak stress in tension, it is forced to enter a softening regime instead of immediate failure. During softening, the bond stresses are reduced, and the bond is allowed to elongate up to a

* Corresponding author: mehdi.alam@student.unimelb.edu.au

certain maximum length (l^*) depending on the critical bond length at peak stress (l_c) given by Eq. 2.

$$l^* = l_c(1 + \alpha) \quad (2)$$

It can be seen the bond length is controlled by a parameter called softening parameter (α) which controls the rate of softening of the bonds. The bond fails once the bond stresses reach below a certain predefined stress which is predefined as a factor of the peak stress. For shear, the bond fails immediately after peak stress is reached [9]. Once the bond fails in either tension or shear, all forces and moments are set to zero and bond parameters are replaced by unbonded contact parameters. There will be some softening that will be observed for the bonds under shear but to keep the number of contact parameters to the minimum, it is assumed that the softening of the bonds in shear will be negligible. The contact parameters for different proportions of the mix are calibrated and validated against 1D compression results observed in the experiments.

2.2 Sample preparation and loading

A cylindrical sample with 50 mm in height and 105 mm in diameter (Fig. 1a) is prepared with the same particle size distribution used in the 1D compression experiments [8] used for validation in the current study (Fig. 1b).

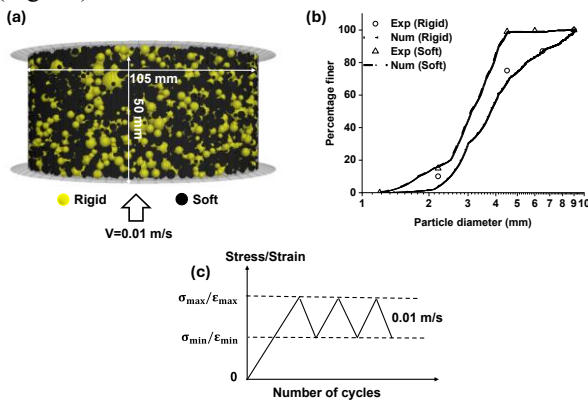


Fig. 1. Sample preparation and loading in DEM (a) prepared sample with dimensions and loading conditions (b) calibration of the particle size distribution with experiments (c) loading-unloading criteria used.

During the sample preparation, a linear contact model is used with zero frictional coefficient for improving the computational efficiency in terms of reducing the unbalanced maximum force at the contact points to negligible. After the sample is prepared with a simple contact model, the contact model, briefly discussed in the previous section, is installed at the contact points. The calibrated normal and shear bonded stiffness is $5 \times 10^{12} \text{ N/m}^3$. The softening factor defined in Eq. 2 is considered to be 2 which means the stiffness of the bonds at the softening stage will be half of the original stiffness. The tensile strength and cohesion for shear strength are defined differently for different contact types. In the next step, all inactive contacts are deleted,

and no new bonded contacts are allowed to form. Instead, if a new contact is formed or a bond breaks, it is assigned with an unbonded contact model. The contact parameters used for the unbonded contacts can be found in previous studies by Alam et al. [2,3]. The samples are then subjected to velocity-controlled cyclic loading with desired maximum and minimum stress/strain levels (Fig. 1c). The maximum and minimum stresses considered for the current study are 1000 kPa and 300 kPa, respectively. In contrast, the strains are varied from 1.5% and 0.6%, respectively, with a maximum allowable velocity of 0.01 m/s to ensure quasi-static loading [10] in each loading and unloading cycle. Quasi-static loading is done to keep the cyclic test in the low-frequency range [11] and prevent higher-frequency effects known to influence cyclic behaviour [12].

3 Results

The effect of stress-controlled and strain-controlled loading is studied here for two different soft content by volume cases (20% and 60%) with a fixed proportion of binder by weight of 4%.

3.1 Strain-controlled loading

Fig 2 illustrates the cyclic response of two granular mixes with different soft content percentages: 20% (Fig. 2a) and 60% (Fig. 2b). The samples are subjected to 30 loading cycles with a minimum and maximum strain of 0.6% and 1.5%, respectively. A clear stress-relaxation effect is observed, characterized by a reduction in vertical stress at both peak strains (ϵ_{max}) and valley strains (ϵ_{min}). The extent of stress-relaxation is notably higher for the mix with 60% soft content (Fig. 2a). In the initial cycles, the 60% soft content mix exhibits greater stress-relaxation compared to the 20% mix. However, for the 20% mix, the rate of stress-relaxation remains relatively constant throughout the cycles. This suggests that stress-relaxation is primarily influenced by bond breakage in the early loading cycles. Once the bond breakage stabilizes, the rate of stress reduction also decreases, as evident in Fig. 2b.

3.2 Stress-controlled loading

3.2.1 Stress-strain response

To further investigate the behaviour of these mixes under cyclic loading, stress-control tests are performed for 30 cycles between stress levels of 1000 kPa and 300 kPa for soft contents of 20% (Fig. 2c) and 60% (Fig. 2d). A clear accumulation of strain with each loading and unloading cycles can be observed for both the soft content cases which is discussed in the next section. Higher strain accumulation at 60% is primarily due to increased bond breakage during the initial loading cycles, resembling the stress-relaxation behaviour observed in strain-controlled loading.

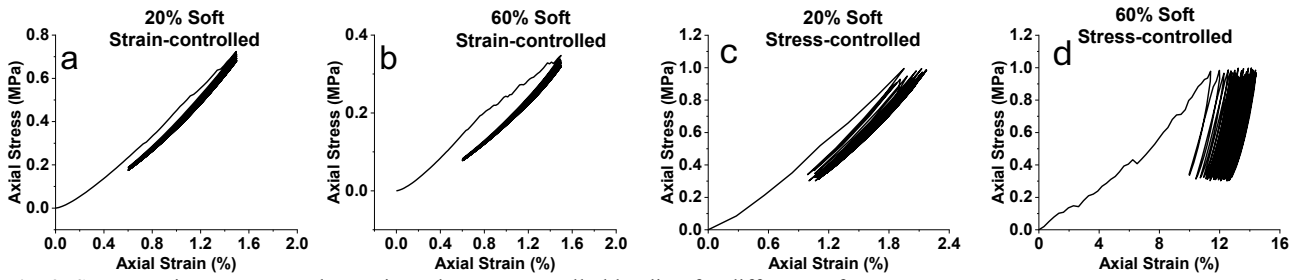


Fig. 2. Stress-strain response under strain and stress-controlled loading for different soft content cases.

3.2.2 Strain accumulation

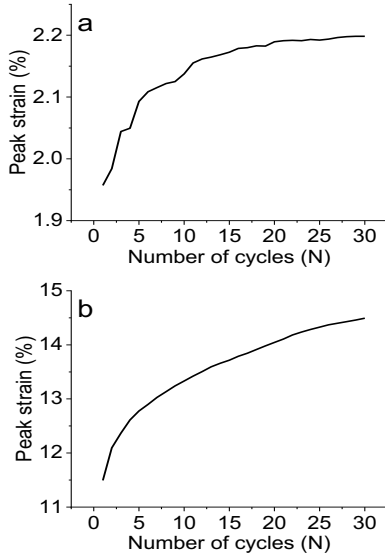


Fig. 3. Strain accumulation for different soft content cases (a) 20% and (b) 60%.

Fig. 3 presents quantification of the accumulated strains for the two different soft content cases. The results indicate that strain accumulation is more pronounced during the initial cycles (ratcheting) before stabilizing at an approximately constant rate. This constant rate is more evident in the mix with lower soft content (Fig. 3a). In contrast, for the mix with higher soft content, strain accumulation remains significant even at higher loading-unloading cycles. When comparing the initial cycles, the mix with higher soft content exhibits a greater strain accumulation rate (Fig. 3b).

4 Discussions

4.1 Modulus degradation

The stress-strain behaviour of geomaterials is inherently non-linear, with true linearity occurring only at very low strain levels. To account for this non-linearity in numerical analysis, a mathematical formulation is proposed to describe the modulus evolution with the number of cycles for both stress- and strain-controlled loading. The proposed equations follow a simple logarithmic function of the number of cycles and require only the constrained modulus and stresses from the first loading cycle. It should be noted that the difference in modulus values between stress-controlled and strain-controlled loading arises from the fact that the tests are

conducted at high and low stress/strain levels, respectively, to capture the response of the mixes over a wider strain range to understand how bond breakage influences the stress-strain behaviour.

4.1.1 Strain-controlled loading

The change in the modulus with each cycle of loading-unloading is plotted for two different soft contents of 20% (Fig. 4a) and 60% (Fig. 4b). A logarithmic function can be fitted for constrained modulus (M) varying with number of cycles (N) for the following curves:

$$M = -(\sigma_{min})_1 \ln(N) + M_1 \quad (3)$$

where, $(\sigma_{min})_1$ and M_1 denote the minimum stress (stress corresponding to minimum strain) the constrained modulus during the first cycle of loading-unloading respectively.

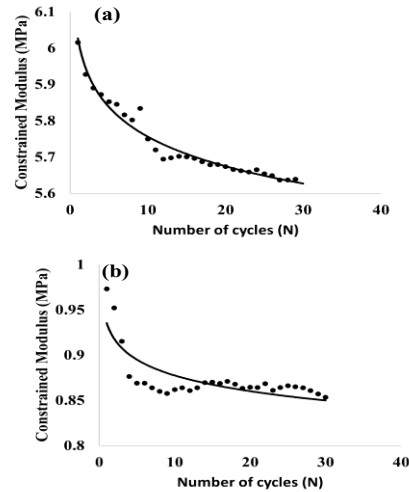


Fig. 4. Variation of modulus with number of cycles for strain-control loading for different soft content cases (a) 20% and (b) 60%

4.1.2 Stress-controlled loading

A similar modulus degradation function from the modulus degradation curves for two different soft contents of 20% (Fig. 5a) and 60% (Fig. 5b) with number of cycles is also proposed for stress-controlled loading and is given by:

$$M = -\sigma_{max} \ln(N) + M_1 \quad (4)$$

where, σ_{max} is the maximum stress upto which the sample is loaded (1000 kPa for the current study).

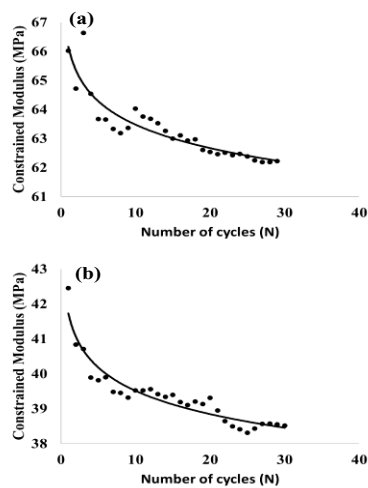


Fig. 5. Variation of modulus with number of cycles for strain-control loading for different soft content cases (a) 20% and (b) 60%

5 Conclusions

In this study, cyclic oedometer tests are conducted on three-phase of bonded soft-rigid granular mixes. An improved contact model developed in DEM is utilized, and both stress- and strain-controlled loading is applied to two different mixes containing 20% and 60% soft content by volume. The stress-strain response reveals stress relaxation in strain-controlled tests, while significant strain accumulation is observed in stress-controlled tests. Notably, strain accumulation and stress reduction are more pronounced during the initial cycles compared to later stages of the loading-unloading process. Additionally, simple logarithmic relationships are proposed for stress- and strain-controlled tests, based on the stress and constrained modulus during the first loading cycle. From the modulus reduction curves, it can be said that mixes with low soft content performs better than the high soft content mixes. However, the modulus reduction after few cycles of loading-unloading also stabilises for high soft content mixes and thus can effectively be used for applications where the mix experiences low stresses. This study has practical relevance for field applications involving these materials, such as permeable pavements where cyclic loading is a key factor. The scope of this study can be further extended by exploring a broader range of soft and binder contents to better understand their influence on material behaviour with microstructural response. Additionally, boundary value problems can be solved using the insights gained from the current investigation of bonded soft-rigid mixtures

References

1. J. Zhang, X. Chen, J. Zhang, P. Jitsangiam, Wang X. DEM investigation of macro- and micro-mechanical properties of rigid-grain and soft-chip mixtures. *Particuology*. **55**, 128–39 (2021).
<https://doi.org/10.1016/j.partic.2020.06.002>.

2. M. Alam, A. Das, M.-M. Disfani. Microstructural behaviour of soft-rigid granular mixes under compressive loads: DEM study using coherent contact model. *Comput. Geotech.* **176**, 106749 (2024).
<https://doi.org/10.1016/J.COMP GEO.2024.106749>.
3. M. Alam, A. Das, M.-M. Disfani. Soft-rigid granular mixtures: Role of particle shape and rolling resistance in response under compressive loads. *E3S Web of Conferences*. **544**, 07007, (2024).
<https://doi.org/10.1051/e3sconf/202454407007>.
4. M. Asadi, A. Mahboubi, K. Thoeni, (2018). Discrete modeling of sand-tire mixture considering grain-scale deformability. *Granul. Matter*, **20**, 2 (2018)
<https://doi.org/10.1007/s10035-018-0791-4>
5. C. Lee, H. Shin, J.-S. Lee. Behavior of sand-rubber particle mixtures: experimental observations and numerical simulations. *Int J Numer Anal Methods Geomech* **38**:1651–63 (2014) <https://doi.org/10.1002/NAG.2264>.
6. J.-S. Lee, J. Dodds, J.-C. Santamarina. Behavior of Rigid-Soft Particle Mixtures. *J. Mater. Civ. Eng.* **19**, 179–84 (2007)
[https://doi.org/10.1061/\(ASCE\)0899-1561\(2007\)19:2\(179\)](https://doi.org/10.1061/(ASCE)0899-1561(2007)19:2(179)).
7. C. Lee, Q.-H. Truong, J.-S. Lee. Cementation and bond degradation of rubber-sand mixtures. *Can. Geotechn. J.* **47**, 763–74 (2010)
<https://doi.org/10.1139/T09-139>
8. R. Raeesi, A. Soltani, M.-M. Disfani. Compressibility Behavior of Soft-Rigid Granular Mixtures Bound with Polyurethane Binder. *Int. J. Geomech.* **22**, 04021265 (2022)
[https://doi.org/10.1061/\(ASCE\)GM.1943-5622.000223](https://doi.org/10.1061/(ASCE)GM.1943-5622.000223)
9. M. Alam, A. Das, & M.-M. Disfani, (2025). Numerical Simulation of Flexible-Bonded Granular Assembly Using DEM., *IOP Conf. Ser.: Earth Environ. Sci.* **1480**(1), 012097.
<https://doi.org/10.1088/1755-1315/1480/1/012097>
10. F. Da Cruz, S. Emam, M. Prochnow, J.-N. Roux, Chevoir F. Rheophysics of dense granular materials: Discrete simulation of plane shear flows. *Phys Rev E Stat Nonlin. Soft Matter Phys.* **72**, 021309 (2005)
<https://doi.org/10.1103/PHYSREVE.72.021309>
11. A.-S.J. Suiker, E.-T. Selig, R. Frenkel Static and Cyclic Triaxial Testing of Ballast and Subballast. *J. Geotech. Geoenvironmental Eng.-ASCE* **131**, 771–82, (2005)
[https://doi.org/10.1061/\(ASCE\)1090-0241\(2005\)131:6\(771\)](https://doi.org/10.1061/(ASCE)1090-0241(2005)131:6(771))
12. Q. Sun, B. Indraratna, N.-T. Ngo. Effect of increase in load and frequency on the resilience of railway ballast. *Geotechnique* **69**, 833–40 (2019)
<https://doi.org/10.1680/JGEO.17.P.302>